

# An approach for calibration of a combined RGB-sensor and 3d camera device

M. Schulze

Institute of Photogrammetry and Remote Sensing  
Technische Universität Dresden, Helmholtzstr. 10, D-01062 Dresden, Germany

## ABSTRACT

The fields of application for 3d cameras are very different, because high image frequency and determination of 3d data. Often, 3d cameras are used for mobile robotic. They are used for obstacle detection or object recognition. So they also are interesting for applications in agriculture, in combination with mobile robots. Here, in addition to 3d data, there is often a necessity to get color information for each 3d point. Unfortunately, 3d cameras do not capture any color information. Therefore, an additional sensor is necessary, such as RGB plus possibly NIR. To combine data of two different sensors a reference to each other, via calibration, is important. This paper presents several calibration methods and discuss their accuracy potential. Based on a spatial resection, the algorithm determines the translation and rotation between the two sensors and the inner orientation of the used sensor.

**Keywords:** calibration, 3d camera, RGB-sensor

## 1. INTRODUCTION

In applications such as mobile robotics, range cameras offer many advantages compared to established devices such as laser scanners or stereo-cameras. An important advantage is their mono-sensorial simultaneous of data capture. The applied 3d camera has a frame rate of 25Hz and a spatial resolution of  $204 \times 204$  pixel. These specifics make this type of sensor suitable for observing dynamic processes in 3d or acquisition of data from mobile platforms. Mobile robots may also be of interest in applications in agriculture, e.g. in precision farming. In addition, color information for each 3d point, like RGB and possibly NIR, is often required for these tasks, because it facilitates the segmentation and classification of the images into plants and background. Furthermore, it is also useful to distinguish plants into plants, which are to be harvested, and obstacles, which need to be circumvented.

Common 3d cameras are not able to capture color data. Therefore, it is necessary to combine a 3d camera and a RGB-sensor to obtain to obtain colored 3d data. A rigorous system calibration is needed to be able to determine the correct color for each 3d point. This paper will present four calibration methods and discusses their potential accuracy. Based on a spatial resection and a bundle adjustment, the algorithms determine translation and rotation parameters between the two sensors and the parameters of interior orientation of the employed sensors. With the collinearity equation and the calculated orientation parameters, it is possible to compute the 2D-position on the RGB-sensor for each 3d point to assign the related color information.

The developed calibration principles can be divided into two categories. Type one works with the 3d camera treated as *passive*. *passive* 3d camera means, only the 2D intensity data of 3d camera is used for calibration, i.e. the 3d camera acquires no 3d points directly. In this case, the relative orientation parameters between the two devices are determined in a bundle block adjustment with multiple images of the 3d camera and the RGB camera. Type two makes more use of the capabilities of the 3d camera. The 3d camera is employed here in an active way to obtain 3d data for calibration. Methods based on single 3d point or 3d object tracking are developed to estimate calibration data. If a single 3d point is tracked, the target is identified via an ellipse fit<sup>1</sup> in two images. After finding more than three corresponding points, the algorithm is able to estimate parameters

---

Further author information:

Marc Schulze: E-mail: marc.schulze@tu-dresden.de, Web: <http://www.tu-dresden.de/ipf/photo/>

of relative orientation  $(X_T, Y_T, Z_T, \omega, \varphi, \kappa)$ . Further methods work with 3d objects to improve 3d point accuracy. The advantage of them is to fit known 3d objects into a 3d point cloud and get an adjusted 3d position. In comparison to a planar ellipse fit, 3d objects increase the depth accuracy of 3d points. High redundancy 3d models achieve a better 3d point accuracy than single points or 2d adjustments. 3d objects can be spheres, edges or corners because they can easily be found in images. For these objects, many single points of 3d camera are used to estimate the parameters of it. For instance, you are able to calculate different planes and intersect them to receive an edge or a corner. Redundancy of a 3d model and the known geometry model of spheres and planes can be used to find outliers and improve the accuracy of a 3d object the accuracy of calculated edges and corners are often better than that of a single 3d point. Some problems of capturing planes are multi path effects and scattering. Multi path effects occur when rays multi reflected from plane surfaces.<sup>2</sup> Scattering badly influenced the distance measurements caused by multiple reflections inside the camera device.<sup>3</sup> So another type of 3d object should be used to avoid these problems. Spheres also allow finding corresponding points on two sensors, and it is possible to interpolate the distance values of it. Errors such as multi-path or scattering are smaller or not existing with this configuration.

## 2. RELATED WORK

One of basic elements of this work is the 3d camera. Principle function and basics of 3d cameras are often illustrated and can be found at following sources: Kahlmann,<sup>4</sup> Gut,<sup>2</sup> and Weingarten.<sup>5</sup> In addition to the principle, there are discussed distance measurement problems caused by temperature, color, material and many more. It offers useful hints to minimize distance errors. A camera calibration of 3d camera is required to improve the captured 3d data. Authors, who discuss this topic are Westfeld<sup>6</sup> and Kahlmann et al.<sup>7</sup>

The fusion of a RGB and a range sensor is the main task of this work. In summary a calibration for relative orientation between these sensors is required. Papers of Ellikide et al.,<sup>8</sup> El-Hakim et al.,<sup>9</sup> Reulke,<sup>10</sup> Prasad et al.,<sup>11</sup> and Guðmundsson et al.<sup>12</sup> deliver approaches, but some of them are difficult to use and very error-prone. Most of them works with multiple images and bundle block adjustments without using 3d data of 3d camera for calibration. Therefore, this paper present four various approaches for relative orientation of RGB camera and range camera.

## 3. SENSOR AND DATA

In this experimental configuration, two different kinds of sensor are used. On the one hand, there is an ordinary RGB camera with a Charged Coupled Device (CCD); it is capturing only color information. A Photon Mixed Device (PMD), on the other hand, is used to determine 3d data.

### 3.1 3D CAMERA

PMD sensors, a main component of 3d cameras, are based on phase shift measurements of modulated light. As a result, it suffers from ambiguity problems. Because only one frequency is used, the solution has to be found within the first wavelength and the range is limited to  $7m$ .

The non-sequential data acquisition mode together with the high frame rate can be seen as the advantage of 3D-cameras over stereo camera systems and laser scanners. Range and intensity values for each pixel of  $204 \times 204$  pixel sensor were saved simultaneously.

PMD Technology,<sup>13</sup> a 3d camera producer, developed the employed 3d camera PMD CamCube 2.0 (Table 1).

### 3.2 RGB CAMERA

A low cost standard RGB camera (Logitech C200 Table 2) is used, in this experiment. The small resolution of  $640 \times 480$  pixel is large enough for fusing with PMD. Because of low frame rate of PMD, 30 frames per second are acceptable for applied RGB camera.

Table 1. Data sheet PMD CamCube 2.0<sup>13</sup>

Parameter	Value
Camara Type	PMD CamCube 2.0
Measurement Range	0.3 to 7 m
Repeatability ( $1\sigma$ )	<3 mm
Frame Rate (3d)	25 fps
Illumination Wavelength	870 nm
Sensor Size	204x204 pixel

Table 2. Specifications of Logitech C200<sup>14</sup>

Parameter	Value
Camara Type	Logitech C200
Frame Rate	30 fps
Sensor Size	$640 \times 480$ pixel

#### 4. METHODOLOGY

The result of this work will be a true color coded 3d point cloud. Therefore, a data fusion of CCD and PMD sensor is essential. This paper deals with some approaches to estimate parameter of relative orientation. They can be divided in two different types. The first type, works with a 3d camera treated as simple 2d imaging sensor; relative orientation is calculated by bundle block adjustment with multiple images of 3d camera and RGB-camera. Herein, only the 2D-intensity images of 3d camera are used for calibration. Therefore, 3d data for relative orientation are calculated by bundle block adjustment. Second type, is more interesting, because it is using the capabilities of 3d camera. It is applied in an active way and 3d points of range camera are used for calibration. Approaches, which are use this kind of type, obtain 3d points from 3d camera and estimate calibration parameters  $(X_T, Y_T, Z_T, \omega, \varphi, \kappa)$  via spatial resection. Furthermore, there is the possibility to fit 3d data to a 3d object. The large number of 3d points can be used to create a high redundancy model, such as planes or spheres. In a adjustment, based on RANSAC<sup>15</sup> and method of least squares, the single point accuracy can be increased. As a result, the 3d position of a 3d object will be improved because of 3d point redundancy and a following adjustment.



Figure 1. Sensor configuration. PMD CamCube and RGB camera Logitech C200 on top.

#### 4.1 CALIBRATION WITH *PASSIVE* 3D CAMERA

The first method, is a offset calibration via bundle block adjustment which use multiple images of miscellaneous point of views. It is often applied and there are various software packages, e.g. AICON,<sup>16</sup> which facilitate computation. In this method, as can be seen in Fig.2, a 3d camera is applied as simple 2D-camera and only intensity images are used. A minimum number of observations is required, therefore there have to be a corresponding number of images. A combination of spatial intersection and spatial resection allows to estimate 3d points, and parameters of the interior and outer orientation of the 3d camera. As a last step, images from a RGB camera and a 3d camera are capture simultaneously. Accordingly, it is possible to estimate parameters of relative orientation between a RGB camera and a 3d camera, with spatial resection.

This kind of sensor calibration uses the 3d camera in a *passive* way because 3d point estimation is done by bundle block adjustment with related 2d points in.

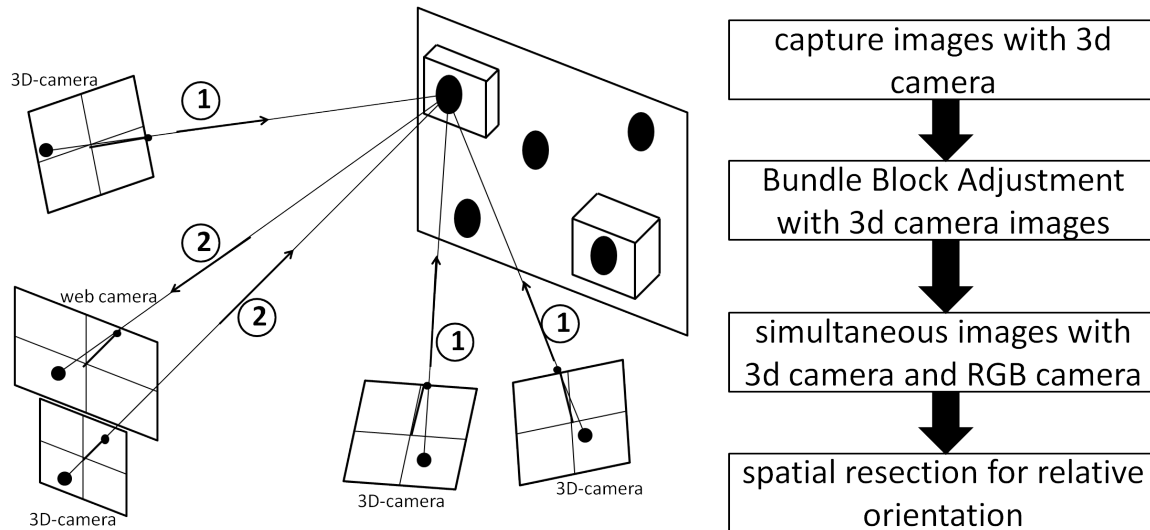


Figure 2. In method 'calibration with passive 3d camera', 3d points were calculated via bundle block adjustment with intensity images of 3d camera.

#### 4.2 CALIBRATION WITH *ACTIVE* 3D CAMERA

In contrast to approach one, as described in section 4.1, this method uses the 3d camera in an active way. It is based only on a spatial resection, but it needs a calibrated 3d camera as a constraint. A calibrated 3d camera is necessary because high accurate 3d points are needed. The procedure, shown in Fig. 3, is divided in three steps. First, feature points in intensity image are found and their 3d points are estimated; second, corresponding feature points in RGB image are search and found using descriptors of SURF;<sup>17</sup> third, the parameters of relative orientation between both cameras are determined via spatial resection.

#### 4.3 CALIBRATION WITH PLANES

An alternative approach, in contrast to section 4.1 and section 4.2, is shown in the next two sections. Because fit of 3d objects to noisy point cloud improve the accuracy of object position, it is better to work with 3d objects instead 3d single points. Hence, there are present two approaches, which apply planes or spheres.

To use the approach with planes, planes have to be found firstly in object space and edges in image space. The developed method employs an approach presented in Guðmundsson,<sup>18</sup> based on finding planes and intersection lines. First, small patches as planes are applied, such as  $15 \times 15$  pixel, of regular 3D point grid and normal vectors are estimated of it. Second, Cartesian normal vectors are transformed in spherical coordinates ( $\varphi$  and  $\theta$ ) and related vectors are merged. Merged normal vectors represent the largest and best detected planes. Third, planes

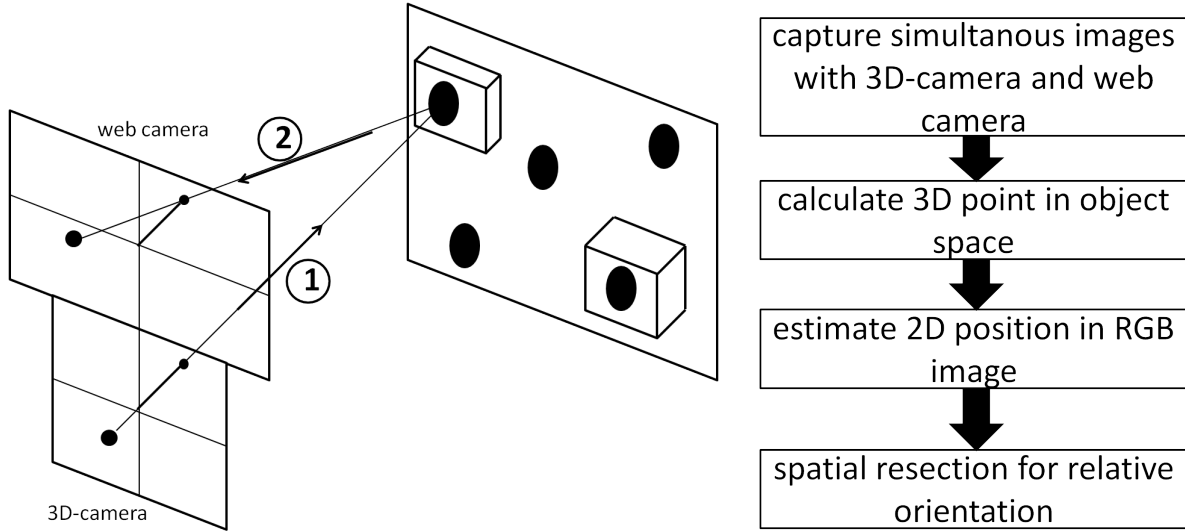


Figure 3. Method 'calibration with active 3d camera' use calculated 3d data of 3d camera. Sensor offset calibration is estimated by spatial resection.

with most probably normal vectors are detected by RANSAC<sup>15</sup> in whole 3d point cloud. Fourth, identified planes are intersect by each other to obtain necessary intersection lines. In a further step, images lines and object lines are referenced to each other. This step is very complex and at the moment only a part of future work (sec. 6). The problem of correspondence can be solved by analyzing the pattern of edge points or an 2d interest closing point algorithm. This assignment is the base for image orientation and a following relative orientation of sensors. An approach of Meierhold and Schmich,<sup>19</sup> which deals with 2D images and laser scanner data, shows the coherence of 3d line parameters and 2d points between two sensors.

$$\begin{aligned}
 x &= x_0 - c \cdot \frac{r_{11} \cdot (X - X_0) + r_{21} \cdot (Y - Y_0) + r_{31} \cdot (Z - Z_0)}{r_{13} \cdot (X - X_0) + r_{23} \cdot (Y - Y_0) + r_{33} \cdot (Z - Z_0)} + dx \\
 y &= y_0 - c \cdot \frac{r_{12} \cdot (X - X_0) + r_{22} \cdot (Y - Y_0) + r_{32} \cdot (Z - Z_0)}{r_{13} \cdot (X - X_0) + r_{23} \cdot (Y - Y_0) + r_{33} \cdot (Z - Z_0)} + dy
 \end{aligned} \tag{1}$$

$$\text{with } \begin{pmatrix} X \\ Y \\ Z \end{pmatrix} = \begin{pmatrix} X_s \cos \alpha \cos \theta - Y_s \sin \alpha + t \cos \alpha \sin \theta \\ X_s \sin \alpha \cos \theta + Y_s \cos \alpha + t \sin \alpha \sin \theta \\ -X_s \sin \theta + t \cos \theta \end{pmatrix}$$

where  $r_{ij}$ : elements of rotation matrix  
 $c, x_0, y_0$ : interior orientation  
 $dx, dy$ : imaging errors  
 $x, y$ : coordinates of image point  
 $X_s, Y_s$ : positional line parameters  
 $\alpha, \theta$ : orientation line parameters

#### 4.4 CALIBRATION WITH SPHERES

A further method to improve the 3d position of objects, such as is section 4.3, is a calibration using spheres. There are some problems using planes for calibration and it is better to apply spheres. Planes evoke multi path effects of radiated illumination on plane surfaces, therefore spheres are more suitable calibration objects. As a result, distance errors occur in the data, which impede the following plane detection step and render an accurate calibration impossible.

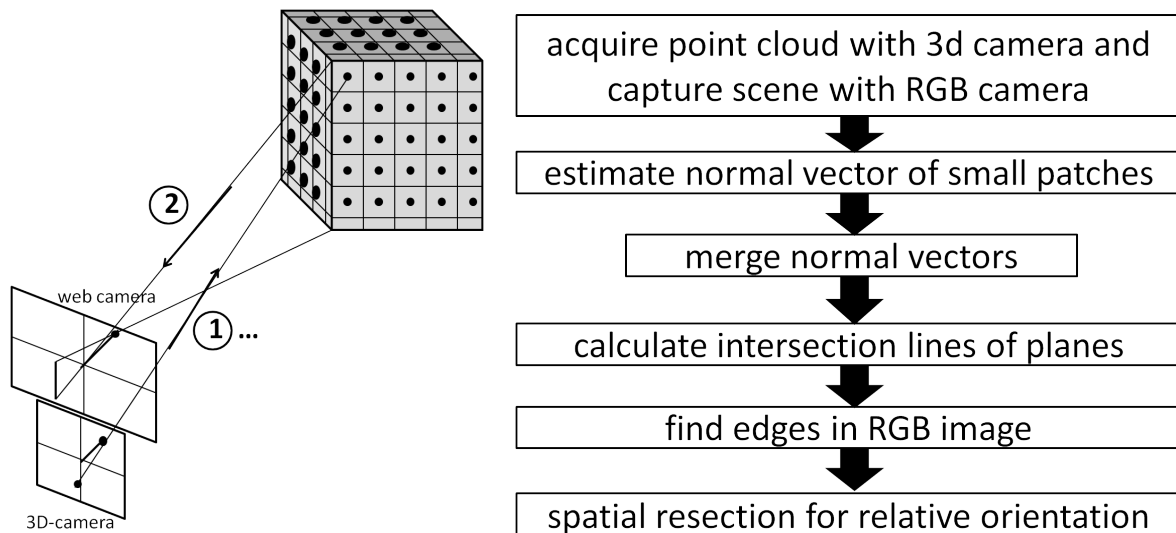


Figure 4. Sensor orientation in assistance with planes. Based on a plane detecting algorithm, intersection lines will be calculated. After a edge detection in RGB camera image, a line assignment between 2D and 3d data is necessary.

One possibility is to use spatial defined and spatial limited objects, like spheres. So it is possible to estimate a 3d position for this object without further intersections or other calculations. Spheres have no plane areas; accordingly there are no problems with multi path errors. Main task of this approach is to detect spheres in object space, find circles in image space, and determine the reference from 3d camera to RGB camera.

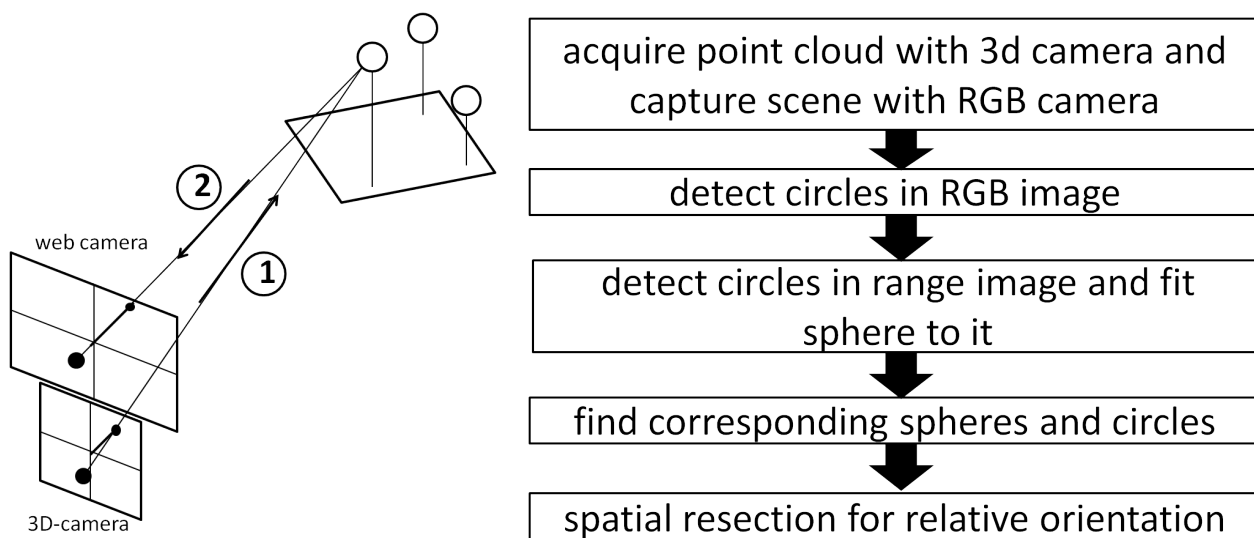


Figure 5. Experimental configuration for sensor calibration, with spheres. Finding spheres in range image and get position of it, while using LSM. Furthermore, finding circles in image space and get orientation between range camera and RGB camera, using circle sphere affiliation.

## 5. RESULTS

In this paper, four approaches for calibration of a RGB camera and range camera have been presented. The advantages and drawbacks of these approaches are discussed in this section.

## 5.1 CALIBRATION WITH *PASSIVE* 3D CAMERA

Using the 3d camera as a 2D-camera is one simple possibility to get 3d data via bundle block adjustment, but it does not use the high potential of it. In spite of this fact is this approach a possible solution to estimate the relative orientation of two sensors because of high accurate 3d point calculation. With this type of calibration, a lot of convergent images are required. The minimum number of required images depends on the number of unknowns. In case of 3d point estimation ( $X_P, Y_P, Z_P$ ) and camera calibration ( $X_0, Y_0, Z_0, \omega, \varphi, \kappa, c, x_H, y_H$ , and seven parameter of distortion), at least eight images are needed. If the camera is already calibrated, at least two images for 3d data estimation are needed. Because of high redundancy, sub-pixel point measurement routines and bundle block adjustment, there is a high accuracy of 3d points. As can be seen in table 3, the average standard deviation of a single point is below  $0.01mm$

In a bundle block adjustment, a least squares method is applied to improve all 3d points and camera parameters. Estimated 3d points are the base for the calibration of relative orientation. Furthermore, the scene or test field with 3d points is captured by a RGB camera. If the RGB-camera is already calibrated, there is only one image necessary for offset estimation, but it depends on the number of 3d points. If the interior orientation of the RGB-camera needs to be calibrated as well, more images are required to determine the unknown of interior orientation.

After the relation of the 3d points to the 2d points on the web cam image are determined, a spatial resection adjustment can be computed to obtain the relative orientation. Based on the highly accurate 3D-points computed by the bundle block adjustment, the resection results for translation parameters are below  $1mm$  and less than  $0.1^\circ$  for rotation parameters (Tab. 4). The results of the resection are illustrated in figure 6 as a correctly colored point cloud. 3d points outside the overlapping area have no color information and painted white.

Table 3. Average standard deviation of single 3d point after bundle block adjustment

$\bar{\sigma}_X$ [mm]	$\bar{\sigma}_Y$ [mm]	$\bar{\sigma}_Z$ [mm]
0.02	0.015	0.025

Table 4. Standard deviation of transformation for calibration with *passive* 3d camera

$\sigma_X$ [mm]	$\sigma_Y$ [mm]	$\sigma_Z$ [mm]	$\sigma_\Omega$ [°]	$\sigma_\varphi$ [°]	$\sigma_\kappa$ [°]
0.7	0.6	0.3	0.03	0.04	0.01

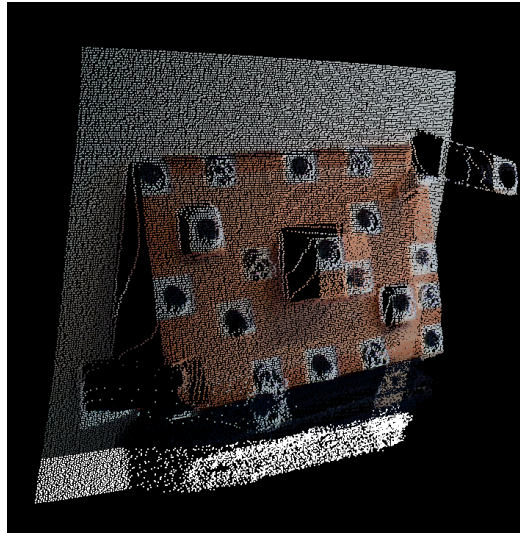


Figure 6. True color coded 3d point cloud. 3d data of range camera with color information of oriented RGB camera.

## 5.2 CALIBRATION WITH ACTIVE 3D CAMERA

A crucial advantage of range cameras are pixel wise distance measurements on the sensor. Thus, a complex configuration, discussed in section 4.1, is actually unnecessary. Instead, sub-pixel image processing routines, e.g. ellipse fitting, are used to compute the position of 3d points in a range image. But, the single point accuracy of PMD is much higher than  $1mm$ . Consequently it is higher than 'Calibration With *Passive* 3d Camera' (cp. Tab. 3). Because of this fact, the results of spatial resection with this configuration cannot be better than the approach presented in section 5.1.

The standard deviation for range values of a single point (PMD CamCube 2.0) is around  $5mm$ , after calibration. Without calibration, single points are not precise enough and the results of the resection are insufficient (Tab. 5).

First of all, z-coordinate is very inaccurate, because the range accuracy is insufficient. To increase the accuracy of single points and further the accuracy of the resection, methods such as plane fitting (Sec. 4.3) and sphere fitting (Sec. 4.4) was developed.

Table 5. Standard deviation of transformation for calibration with *active* 3d camera

$\sigma_X$ [mm]	$\sigma_Y$ [mm]	$\sigma_Z$ [mm]	$\sigma_\Omega$ [°]	$\sigma_\varphi$ [°]	$\sigma_\kappa$ [°]
3.0	4.9	15.8	0.46	0.22	0.57

## 5.3 CALIBRATION WITH PLANES

In our approach, the main aim is the improvement of the single point measurements captured by range camera. Therefore, a geometric model, especially planes, with high redundancy is used. The geometric model of a plane (Eq. 2) is described by three unknowns, the parameter of the normal vector  $(X_N, Y_N, Z_N)$ .

$$d = \begin{pmatrix} X_N \\ Y_N \\ Z_N \end{pmatrix} \cdot \begin{pmatrix} X \\ Y \\ Z \end{pmatrix} \quad (2)$$

It requires at least three 3d points to compute this unknowns of a plane. If there are more than three 3d points, a redundancy is given and an adjustment provides the best solution of unknowns. To avoid outliers and following errors, a RANSAC<sup>15</sup> algorithm is implemented to obtain the best parameters of plane.

As a first step, planes are searched in range image. An algorithm, based on an approach presented by Guðmundsson,<sup>18</sup> was developed to detect planes. It calculates normal vectors of small user defined patches (e.g.  $7 \times 7$  or  $15 \times 15$  pixel). Because of noise in the range measurements, a RANSAC is used algorithm for robust detecting of planes. Following, the Cartesian normal vectors ( $\vec{X} = [X, Y, Z]$ ) were transformed to spherical coordinates ( $[\phi, \theta, r]$ ). So, the variables of descriptive direction are reduced from three parameters of normal vector  $(X_N, Y_N, Z_N)$  to two parameters  $(\phi, \theta)$ . Analyzing the behavior of  $\phi$  and  $\theta$ , the values of  $\phi$  contain all important information. As a result, it is possible to find all corresponding planes with only one parameter,  $\phi$ .

Next, planes with similar  $\phi$  directions within a tolerance of  $10^\circ$  were merged and all large planes of the image are obtained. For detecting edges, planes have to intersect to each other. These intersection lines present all identified edges in object space and are assigned to their corresponding lines in the RGB image.

Detecting edges in object space and establishing correct line correspondence is a difficult and error-prone procedure. Finally, this method is only an approach to compute the relative orientation of two sensors. Problems of unknown affiliation of edges in the range image and the RGB image are not solved at the moment and are parts of future work. In spite of this fact, the described approach is a possibility to estimate the relative orientation of two sensors.

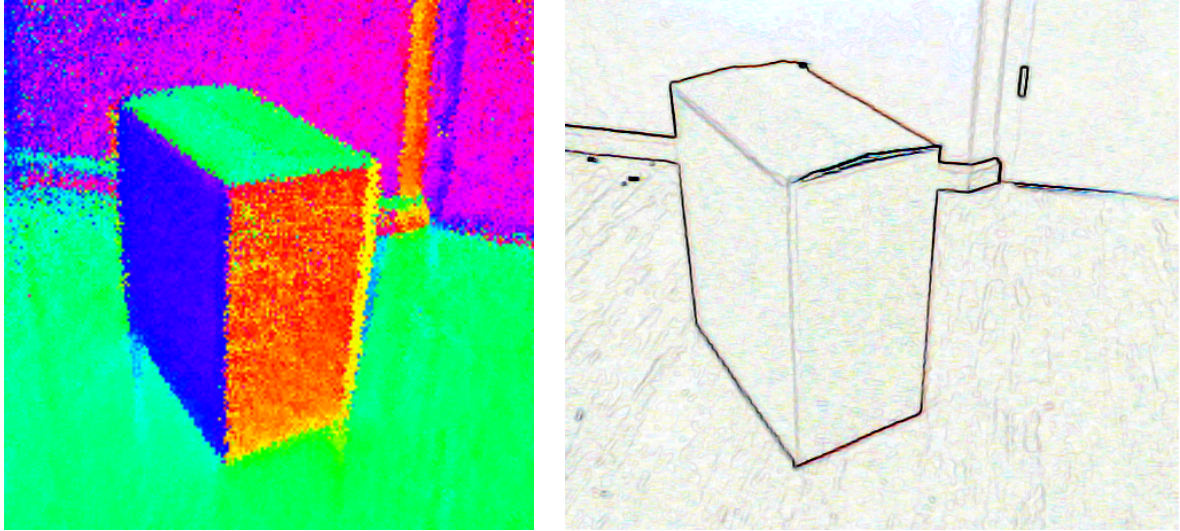


Figure 7. Finding planes, while using RANSAC. On the left side, the color coded  $\phi$  image with different plane directions. On the right side, edges of RGB camera image.

#### 5.4 CALIBRATION WITH SPHERES

To avoid a complex configuration and implementation, like in section 5.3, another approach was developed. As mentioned in section 4.4, this type of calibration deals with spheres. They were used as geometric objects to increase single point accuracy.

First, finding ellipses in the range image and fitting spheres to the 3d point cloud. Based on RANSAC and a following least squares algorithm, sphere are fitted in a certain position. The four unknown parameters of a sphere are offset from origin ( $X_M, Y_M, Z_M$ ) and the radius ( $r$ ) (Eq. 3). At least four points are needed to obtain a unique solution. If there are more than four points, a redundancy is given and an adjustment is necessary.

$$r^2 = (X - X_M)^2 + (Y - Y_M)^2 + (Z - Z_M)^2 \quad (3)$$

As can be seen in table 6, the 3d position could be increased about 25 times, in comparison to 5mm single point standard deviation. This improvement could be raise the accuracy of spatial resection, because it depends on single point measurement accuracy. Following, ellipses in RGB image are connected to corresponding spheres of object space. The problem of affiliation is mentioned in section 5.3 and is a part of future work yet. Identification of correct correspondence is the base for spatial resection. Therefore, related 3d coordinates of spheres and 2d coordinates ellipses are needed.

Table 6. Average standard deviation of sphere center

$\bar{\sigma}_X [mm]$	$\bar{\sigma}_Y [mm]$	$\bar{\sigma}_Z [mm]$
0.19	0.18	0.28

#### 6. CONCLUSION AND FUTURE WORK

In this paper four approaches for calibration of a range sensor and a RGB camera have been shown. The well known method of bundle block adjustment delivers highly accurate results, but it is complex computation and requires more than one convergent image. If the implementation of this adjustment is given, it is a simple way to estimate parameters of relative orientation. Other developed configurations have their advantages and disadvantages in configuration and accuracy. Because of insufficient single point accuracy of range measurements, the calibration calculation is rendered impossible and yields no meaningful results (Sec. 5.2). The improvement

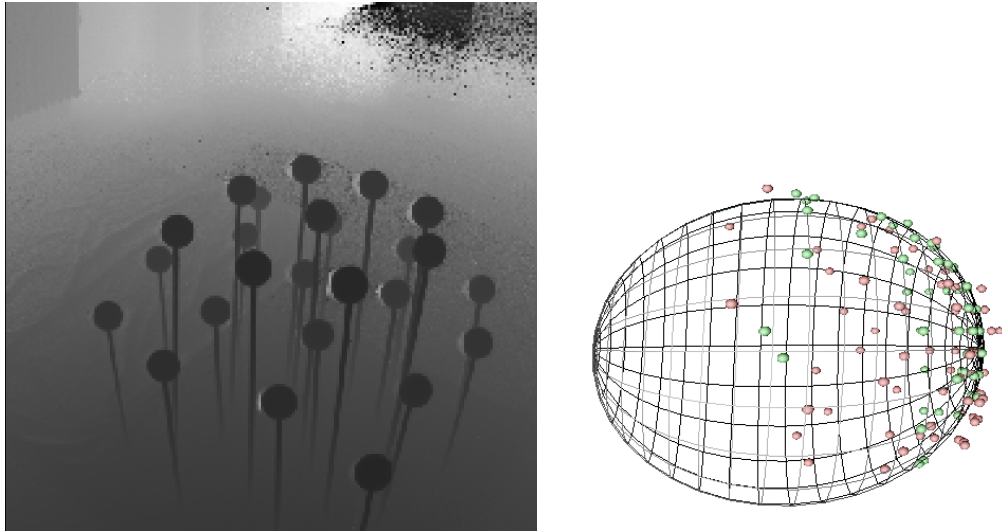


Figure 8. Finding sphere, while using RANSAC and least squares algorithm. On the left side, the range image of test field with spheres. On the right side, valid points, invalid points, and fitted sphere.

of range accuracy via 3d objects can solve the described problems of inaccurate 3d point data. An experimental configuration with planes (Sec. 5.3) is one possibility to achieve a better 3d point accuracy. But, it is difficult to find corresponding lines or edges in image or object space. The results obtained by using spheres 3D-calibration objects produced the most accurate results. Furthermore, spheres facilitate the detection because of ellipse detecting in images and establishing of correspondences. The increased 3d point accuracy, using high redundancy geometric models and adjustments, is the base for an accurate resection.

Future work be engaged with improvements of fourth approach (Sec. 4.4) because it has the most potential to avoid a complex bundle block adjustment (Sec. 4.1) and achieves nearly same results. Further, a solution for problems of affiliation between corresponding points in object space and image space have to be found. It is possible to solve it by feature descriptors, like mentioned in SURF,<sup>17</sup> or by an interest closest point algorithm.

## REFERENCES

1. T. Luhmann, *Nahbereichsphotogrammetrie*, Wichmann Verlag, 2010.
2. O. Gut, “Untersuchungen des 3D-Sensors SwissRanger,” Master’s thesis, ETH Zurich, 2004.
3. *Optimized scattering compensation for time-of-flight camera*, 2007.
4. T. Kahlmann, *Range Imaging Metrology: Investigation, Calibration and Development*. PhD thesis, ETH Zurich, 2007.
5. J. Weingarten, “A state-of-the-art 3d sensor for robot navigation,” tech. rep., Swiss Federal Institute of Technology, 2004.
6. P. Westfeld, “Ansätze zur kalibrierung des range-imaging-sensors sr-3000 unter simultaner verwendung von intensitäts- und entfernungs-bildern,” in *Photogrammetrie - Laserscanning - Optische 3D-Messtechnik, Photogrammetrie - Laserscanning - Optische 3D-Messtechnik*, 2007.
7. T. Kahlmann, F. Remondino, and H. Ingensand, “Calibration for increased accuracy of the range imaging camera swissranger,” in *ISPRS Commission V Symposium 'Image Engineering and Vision Metrology'*, 2006.
8. L.-P. Ellekilde, J. V. Miró, and G. Dissanayake, “Fusing range and intensity images for generating dense models of three-dimensional environments,” tech. rep., ARC Centre of Excellence for Autonomous Systems, Faculty of Engineering, University of Technology Sydney, 2007.
9. S. F. El-Hakim, C. Brenner, and G. Roth, “A multi-sensor approach to creating accurate virtual environments,” *ISPRS Journal of Photogrammetry & Remote Sensing* **53**, pp. 379–391, 1998.
10. R. Reulke, “Combination of distance data with high resolution images,” in *ISPRR Commission V*, 2006.
11. T. Prasad, K. Hartmann, W. Weihs, S. E. Ghobadi, and A. Sluiter, “First steps in enhancing 3d vision technique using 2d/3d sensors,” in *Computer Vision Winter Workshop 2006, Ondrej Chum*, 2006.
12. S. Guðmundsson, H. Aanæs, and R. Larsen, “Fusion of stereo vision and time-of-flight imaging for improved 3d estimation,” *Intelligent Systems Technologies and Applications* **1**, pp. 164–172, 2007.
13. PMD, “Pmd[vision] camcube 2.0,” 2010. <http://www.pmdtec.com/>.
14. Logitech, “Logitech c200,” 2010. <http://www.logitech.com>.
15. M. Fischler and R. Bolles, “Random sample consensus: A paradigm for model fitting with applications to image analysis and automated cartography,” *Communications of the ACM* **24**, pp. 381–395, 1981.
16. Aicon, 2011. <http://www.aicon.de>.
17. H. Bay, A. Ess, T. Tuytelaars, and L. V. Gool, “Speeded-up robust features (surf),” *Vision and Image Understanding (CVIU)* **110(3)**, pp. 346–359, 2008.
18. S. A. Guðmundsson, “Robot vision applications using the csem swissranger camera,” tech. rep., Technical University of Denmark, 2006.
19. N. Meierhold and A. Schmich, “Referencing of images to laser scanner data using linear features extracted from digital images and range images,” in *ISPRS Com. V Symposium*, 2010.